Quantum Electronics **48** (5) 431–437 (2018)

https://doi.org/10.1070/QEL16653

On the duration of continuous operation of an optical frequency standard based on strontium atoms

O.I. Berdasov, D.V. Sutyrin, S.A. Strelkin, A.Yu. Gribov, G.S. Belotelov, A.S. Kostin, N.N. Kolachevsky, S.N. Slyusarev

Abstract. **This paper examines methods for increasing the duration of autonomous continuous operation of optical frequency standards. We have realised the secondary cooling of strontium atoms without using phase stabilisation during the formation of cooling and intermixing light beams and proposed a clock laser frequency stabilisation algorithm that compensates for the acoustic noise-induced laser frequency instability. Experiments have been performed using two distinct algorithms for laser frequency stabilisation to the frequency of an atomic transition. The maximum duration of continuous autonomous operation of the system was 25 000 to 50 000 s with one stabilisation algorithm and 70 000 to 200 000 s with the other algorithm.**

Keywords: *Sr atom, laser cooling, optical lattice, optical frequency standard, clock transition.*

1. Introduction

More than sixty years ago, Essen [1] demonstrated the first atomic frequency standard, based on the use of the ground-state hyperfine frequency interval of the ^{133}Cs atom [1]. Just ten years after that, the caesium frequency standard (FS) was adopted by the International Committee for Weights and Measures (CIPM) as a primary time and frequency standard. To date, advances in controlling cold atoms have led to the advent of precision optical atomic clocks, which find application in various areas of metrology, navigation and fundamental physics: in studies of the temporal stability of fundamental constants [2–5], to verify Einstein's equivalence principle [6, 7], in searching for dark matter [8], in positioning systems [9] and in very long baseline interferometry [10].

O.I. Berdasov, S.A. Strelkin, A.Yu. Gribov All-Russia Research Institute of Physical and Radio Engineering Measurements, 141570 Mendeleevo, Moscow region, Russia; National Nuclear Research University 'MEPhI', Kashirskoe sh. 31, 123182 Moscow, Russia; e-mail: berd_7@mail.ru;
D.V. Sutyrin, G.S. Belotelov, A.S. Kostin, S.N. Slyusarev All-Russia Research Institute of Physical and Radio Engineering Measurements, 141570 Mendeleevo, Moscow region, Russia;
N.N. Kolachevsky All-Russia Research Institute of Physical and Radio Engineering Measurements, 141570 Mendeleevo, Moscow region, Russia; National Nuclear Research University 'MEPhI', Kashirskoe sh. 31, 123182 Moscow, Russia; P.N. Lebedev Physical Institute, Russian Academy of Sciences, Leninsky prosp. 53, 119991 Moscow, Russia

Received 21 February 2018; revision received 20 March 2018
Kvantovaya Elektronika **48** (5) 431–437 (2018)
Translated by O.M. Tsarev

In terms of relative accuracy and frequency stability, modern optical clocks surpass the best modern caesium fountains by several orders of magnitude. At present, the optical clocks are based on single ions or ensembles of neutral atoms loaded into an optical lattice. The two types of optical clocks are similar in relative frequency uncertainty: 2.1×10^{-18} for optical clocks based on neutral Sr atoms [11] and 3.2×10^{-18} for clocks utilising an octupole (E3) Yb^+ transition [12].

Active development of optical clocks is a prerequisite for redefinition of the second, which is being actively discussed at CIPM [13, 14]. In connection with this, researchers and designers of optical clocks are confronted with several basic problems.

1. It is necessary to evaluate the frequency uncertainty of the optical clocks. For redefinition of the second, the uncertainty of the optical clocks should be lower than that of the caesium optical clocks. At present, the relative frequency uncertainty of the optical clocks based on ^{87}Sr atoms in an optical lattice [11, 15], a single $^{171}Yb^+$ ion (octupole transition) [12] and a single $^{27}Al^+$ ion [16] is at a level of 1×10^{-18}, which is almost two orders of magnitude lower than that of the best caesium fountain [17, 18].

2. The equivalence and reliability of the optical clocks should be put in test. For this purpose, it is preferable to compare optical clocks based on the same particles. At present, many national metrology institutes investigate ^{87}Sr optical clocks and compare them to each other. To this end, optical fibre links were made between PTB (Physikalisch-Technische Bundesanstalt, Germany) and SYRTE (Systèmes de Référence Temps Espace, France) [19] and between RIKEN (Rikagaku Kenkyūsho, Japan) and UT (University of Tokyo, Japan) [15], and a transportable ^{87}Sr optical clock was made at PTB [20].

3. It is necessary to examine the feasibility of using optical clocks as frequency unit keepers for improving the accuracy of TAI, an international atomic time scale. Here, a detailed report is needed on experimental data obtained in certain periods of time, including the set of residual systematic errors, which influence the accuracy of determining the frequency unit. It is necessary to continuously compare optical clocks with a caesium fountain in order to ensure direct connection between the prospective and current definitions of the second.

The first two problems are being successfully resolved by the metrological community, but the last problem involves serious difficulties in ensuring prolonged continuous operation of all optical clock components. It is for this reason that reports in the scientific literature deal primarily with results of continuous studies conducted for only relatively short periods of time. One way to fill time gaps due to breaks in optical

clock operation is to use extrapolation algorithms [21, 22]. Frequency fluctuations in hydrogen masers, used as frequency keepers, during such gaps remain the major frequency uncertainty sources. To avoid such uncertainties, it is necessary to ensure reliable continuous operation of optical clocks for a long time.

In this paper, we describe approaches used by us to ensure prolonged (~24 h) uninterrupted operation of optical clocks based on cold ^{87}Sr atoms. One approach is to abandon phase stabilisation in the optical scheme of secondary cooling of atoms. The other approach is to stabilise the clock laser frequency to the frequency of the ^{87}Sr $^1S_0-{}^3P_0$ transition.

2. Preparation of an ensemble of atoms

To prepare an ensemble of cold atoms necessary for Doppler-free spectroscopy of a clock transition, use is made of a classic approach based on a Zeeman slower and magneto-optical trap (MOT).

The first laser cooling stage employs the ^{87}Sr $^1S_0-{}^1P_1$ transition at $\lambda = 461$ nm in the presence of repumping lasers emitting at $\lambda = 679$ and 707 nm (Fig. 1a). The number of ^{87}Sr atoms in the primary MOT is at least 10^6, with a characteristic temperature from 1 to 3 mK (depending on experimental parameters).

The second laser cooling stage employs the $^1S_0-{}^3P_1$ transition at $\lambda = 689$ nm. Because of its nonzero nuclear spin ($I = 9/2$), the ^{87}Sr isotope has a more complex energy level structure than does the ^{88}Sr isotope, whose secondary cooling was demonstrated previously [23]. For effective secondary cooling of ^{87}Sr atoms, it is necessary to ensure an appropriate population distribution over the sublevels of the $^1S_0$ ground state. For this purpose, use is made of additional, stirring light at the frequency of the $^1S_0(F = 9/2)-{}^3P_1(F' = 9/2)$ transition, whereas the main, cooling light is adjusted to the frequency of the $^1S_0(F = 9/2)-{}^3P_1(F' = 11/2)$ transition. A problem pertaining to secondary cooling is that laser light should simultaneously act on the ^{87}Sr atoms at the frequencies of these transitions, which differ by 1.4 GHz. One way to resolve it is to use two laser sources with a phase stabilisation system for their outputs. However, this may have a negative effect on the reliability of operation on the whole, so for the experimental implementation of the processes described above we built an optical system (Fig. 2) based on a number of acousto-optic modulators AOMs. In combination with 1 °C temperature instability in the laboratory, this allows us to dispense with additional adjustment of the system for long periods of time (of the order of several months), thus ensuring long-time operation.

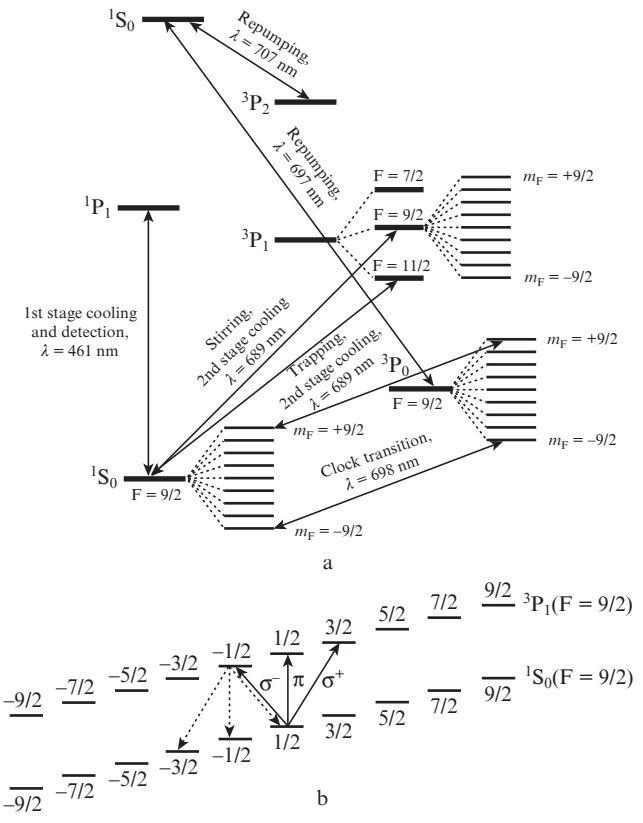

Figure 1. (a) Diagram of the ^{87}Sr transitions involved in the operation of optical clocks and (b) structure of the magnetic sublevels of the $^1S_0$ and $^3P_1$ states in the presence of a static magnetic field.

After the secondary cooling stage, the number of atoms in the MOT is $\sim 10^5$, with a characteristic temperature no higher than 2.5 μK, which allows $\sim 10^4$ atoms to be loaded into the optical lattice at the 'magic' wavelength ($\lambda_m = 813$ nm). The depth of the optical lattice, U_{trap}, can be evaluated from the frequencies of the sidebands of the $^1S_0-{}^3P_0$ clock transition: $U_{trap} \approx 56E_{rec}$ (where E_{rec} is the recoil energy), and the lifetime of atoms in it is 0.5 s.

3. Spectroscopy of the clock transition

The determination of the probability of ^{87}Sr excitation to the $^3P_0$ state involves a few steps that take place within one working cycle. In the first step, atoms interact with a pulse of clock light, whose duration is determined by the Rabi frequency. At a light intensity $I = 0.7$ W cm^{-2}, the experimentally determined π-pulse duration was 70 ms. In the second step, all of the atoms that remain in the $^1S_0$ ground state are recorded and removed from the lattice using a detecting pulse at $\lambda = 461$ nm, corresponding to the $^1S_0-{}^1P_1$ transition. The fluorescence signal is recorded by a 16-bit CCD camera with an electro-optical converter. Next, the atoms in the $^3P_0$ state are brought back to the ground state by repumping laser pulses at $\lambda = 679$ and 707 nm and also recorded by a detecting pulse. The signals from the first (I_1) and second (I_2) detecting pulses are used to determine the probability of excitation to the $^3P_0$ state:

$$P = \frac{I_2}{I_1 + I_2}.$$

Since the ^{87}Sr atom has a nonzero nuclear spin, the spectrum of the $^1S_0-{}^3P_0$ transition comprises 28 lines, corresponding to transitions between magnetic sublevels. To lift the degeneracy of states with different magnetic quantum numbers, use is made of an external static magnetic field induced by MOT coils in a Helmholtz configuration. If the angle between the clock light polarisation vector and the magnetic induction vector is zero, π-transitions are observed, which correspond to a change in magnetic quantum number $\Delta m_F = 0$. The optical lattice is oriented vertically, and its laser light is linearly polarised along the magnetic induction vector of the static magnetic field. The clock laser output is linearly polarised and propagates along the optical lattice axis.

To increase the signal-to-noise ratio in determining the excitation probability P, we used an additional, circularly

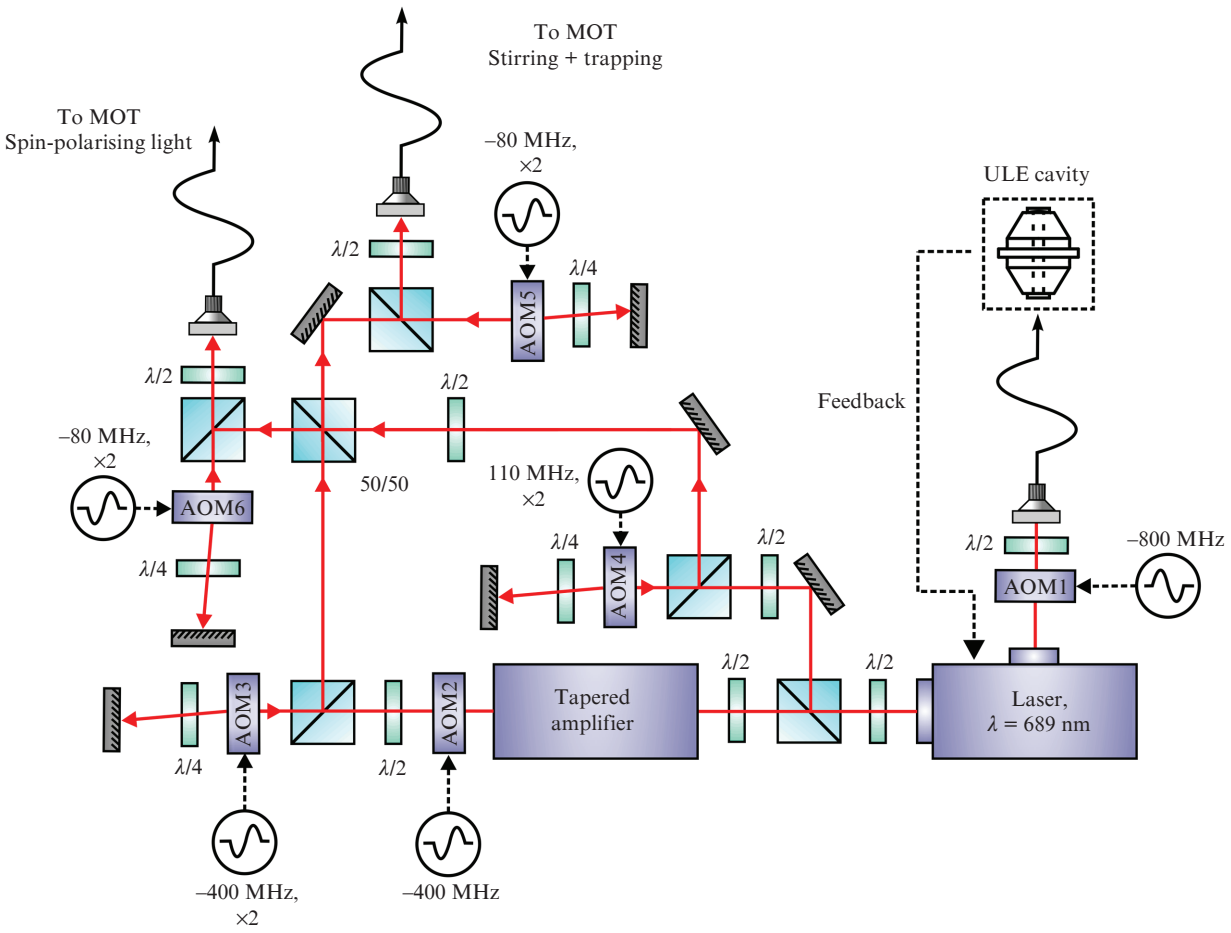

Figure 2. Schematic of the system for the secondary cooling of ^{87}Sr atoms. The symbol '×2' corresponds to the frequency shift as a result of a double pass of the laser light through the AOM, and the symbol '–' corresponds to a negative shift of the laser light as it passes through the AOM.

polarised light with λ = 689 nm, which allowed us to redistribute atoms to states with m_F = –9/2 or 9/2, depending on the choice of the polarisation direction (Fig. 1b). The wave vector of the laser light is then directed along the magnetic induction vector. After the atoms are transferred to one of the above magnetic sublevels, the excitation probability P is determined according to the algorithm described above.

As a laser source for the spectroscopy of the $^1S_0$–$^3P_0$ clock transition, we used a system based on a DL Pro semiconductor laser (Toptica, Germany) and external high-finesse ultra-low expansion (ULE) cavity. The spectral linewidth of such a system is ~1 Hz, the frequency drift is ~91 mHz s^{-1}, and the relative frequency instability with no allowance for the linear drift is $(2–3)\times10^{-15}$ at averaging times from 1 to 100 s [24].

The laser frequency is tuned using the acousto-optic modulator AOM-S (Fig. 3), which is controlled by a program written in the LabVIEW environment. The duration of one working cycle, which involves two laser cooling stages, the loading of atoms into the optical lattice and determination of the excitation probability P is ~1.3 s.

4. Laser frequency stabilisation to an atomic resonance

The clock laser frequency in an optical clock should be stabilised to an ultranarrow line of an atomic transition. In most cases, the error signal for stabilisation is generated by tuning the laser frequency near an atomic resonance and measuring the frequency-dependent probability P of excitation to the upper atomic level $^3P_0$. The operation of an optical clock has a cyclic character due to the necessity of loading atoms into the optical lattice. To stabilise the laser frequency to the clock transition frequency, excitation probabilities P are determined at the laser frequency tuned to below and above the resonance frequency in neighbouring working cycles. The frequency detuning is chosen so as to maximise the slope of the spectral excitation curve and typically approaches the full width at half maximum of the atomic resonance line. This approach is widely used and has been implemented in many laboratories in the world [25–27]. Its drawback, critical in our case, is that such a scheme is unstable to external influences. As we noted previously, acoustic noise (opening of doors in the building, noise, etc.) can lead to short-term disturbances of laser frequencies, which can in turn entail a rather large error in probability determination in a particular cycle. Because of the resultant inaccuracy, a false correction is made to the centre frequency, which may cause inadequate operation of the stabilisation system.

In connection with this, we used a slightly different approach. After preliminarily obtaining the spectrum of the $^1S_0$–$^3P_0$ transition and determining its resonance frequency f_0 and spectral linewidth, we chose a frequency tuning step that allowed the spectrum to be reconstructed using N data points. In the first step, an array is formed that consists of AOM-S frequencies and the corresponding probabilities P of excitation to the upper atomic level. Next, in one imple-

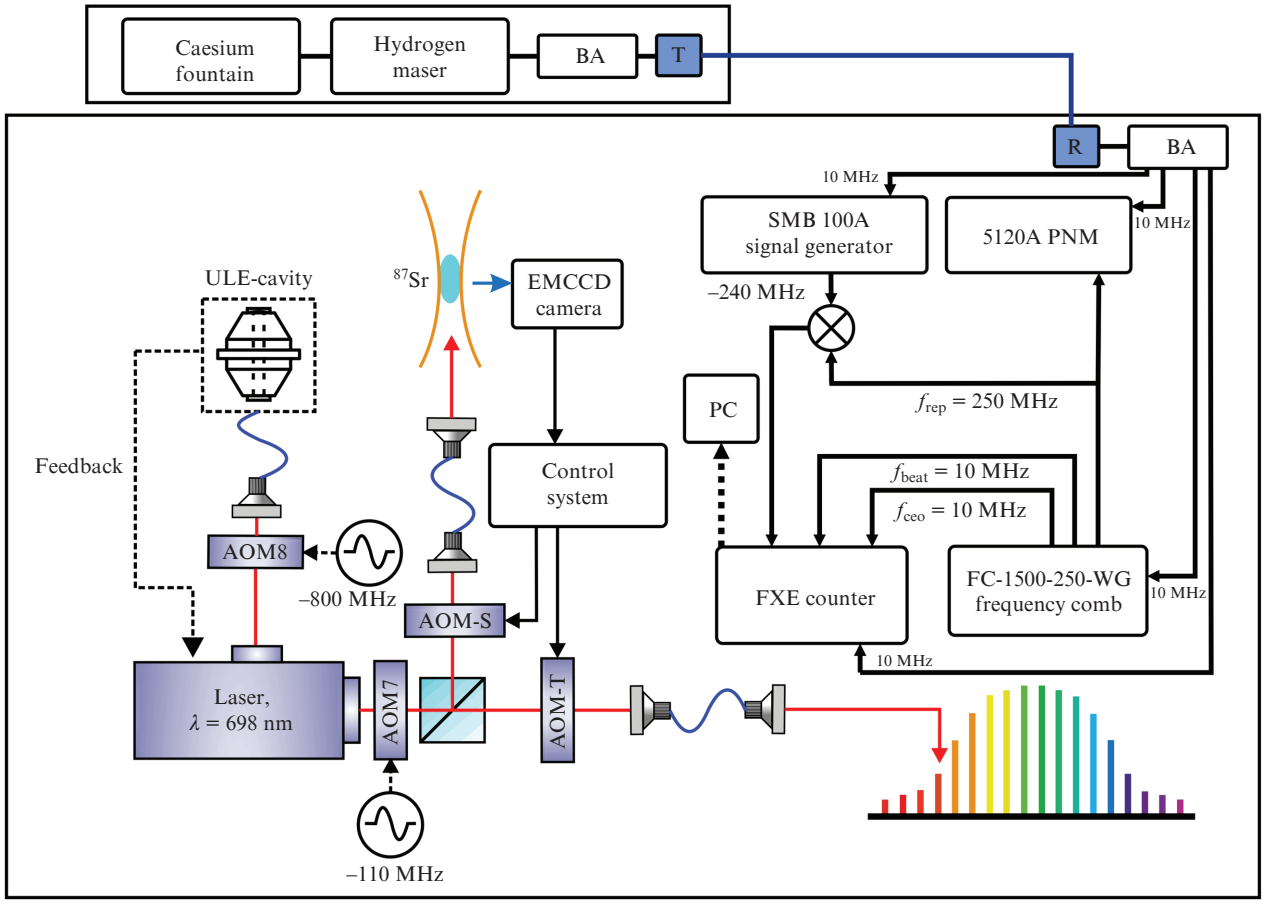

Figure 3. Comparison scheme: (BA) buffer amplifier; (T) optical transmitter for signals at a frequency of 10 MHz; (R) optical receiver for signals at a frequency of 10 MHz; (5120A PNM) phase noise meter; (PC) personal computer; (AOM-T) AOM tuning the clock laser frequency to resonance with the atomic transition frequency; (AOM-S) AOM tuning the clock laser frequency as the atomic transition is scanned; (SMB 100A) RF signal generator.

mentation of the stabilisation algorithm, we determine the frequency $(f_0)_n$ (where n is the number of the working cycle) corresponding to the maximum probability P obtained in the array. The earlier determined resonance frequency P is then corrected: $(f_0)_n = (f_0)_{n-1} + \Delta f$, where $\Delta f = k((f_0)_n - (f_0)_{n-1})$ (k is an empirical coefficient).

In the other implementation, after the spectrum of the excitation probability P is reconstructed, it is fitted with a Lorentzian:

$$P(x) = A\frac{w}{(x - x_c)^2 + w^2},$$

where x is frequency; x_c is the resonance frequency; and A is the area under the Lorentzian. In the case of a rectangular laser pulse of finite duration, the spectrum of the clock transition should contain Rabi oscillations and the expected spectrum should be described by a function of the form $\mathrm{sinc}^2 x$. However, under the experimental conditions of this study, it is a Lorentzian that best describes the spectrum. This is due to an additional broadening of the spectrum, which may originate from the laser noise, the small lifetime of atoms in the lattice, the frequency shift of the laser forming the lattice and the external magnetic field.

The x_c value thus found and its uncertainty Δx_c are used to find the correction of the resonance frequency f_0. If $|x_c - f_0| < p\Delta x_c$ (where p is the confidence interval coefficient to be found experimentally), we have $f_0 = x_c$. Otherwise, f_0 remains unchanged and x_c is redetermined.

This approach has the advantage that the reliability of the obtained data is further verified: excitation probabilities that are obviously inconsistent with the Lorentzian profile are remeasured, which allows one to reduce the effect of external noise (acoustic, electrical, etc.) on the stability of optical clock operation.

After sequentially obtaining spectra of transitions between the magnetic sublevels ($m_F = +9/2 - m_F' = +9/2$) and ($m_F = +9/2 - m_F' = -9/2$) of the $^1S_0$ and $^3P_0$ states and determining their centre frequencies by fitting with Lorentzians, we evaluated their average. The frequency thus obtained, corresponding to the transition between the zeroth magnetic sublevels ($m_F = 0 - m_F' = 0$), was fed to the acousto-optic modulator AOM-T (Fig. 3). In addition to an increase in signal-to-noise ratio, an important advantage of the sequential spectroscopy of symmetric magnetic components in the spectrum of the clock transition, followed by calculation of the average frequency, is the suppression of the linear Zeeman shift of the clock transition frequency.

5. Functioning of the optical clock and comparison with a caesium fountain

In this study, to compare strontium clocks with a caesium fountain, we built a system schematised in Fig. 3. To bring

characteristics of optical clocks to the radio frequency range, part of the output of a laser tuned to the frequency of the $^1S_0$–$^3P_0$ clock transition using AOM-T is used to stabilise a frequency comb. Its spectrum has the form of a set of frequency-equidistant lines in the optical region and is characterised by two parameters: pulse repetition rate f_{rep} and frequency difference between the optical phase and pulse envelope peak, f_{ceo}. They are located in the radio frequency range and can readily be measured by commercially available frequency counters. Thus, the frequency of the clock transition can be determined as

$$\nu_{^{87}Sr} = Nf_{rep} \pm f_{ceo} \pm f_{beat},$$

where f_{beat} is the frequency of beating between the frequency comb mode and the clock laser output and N is the number of the comb mode, which can be determined using a wavemeter with an accuracy better than $\pm f_{rep}/2$.

In our case, we used an FC-1500-250-WG commercially available fibre-optic frequency comb (Menlo Systems, Germany) with f_{rep} = 250 MHz. To stabilise the frequency f_{ceo} using an f–$2f$ interferometer [28], the emission spectrum of the frequency comb is broadened by an octave using a femtosecond fibre amplifier and highly nonlinear fibre. To obtain the beat signal between the femtosecond comb emission and laser output, a femtosecond comb mode at $\lambda \approx 698$ nm is generated by doubling the frequency of a part of its spectrum. The clock laser output is sent to the femtosecond comb through a 10-m-long fibre in the first series of measurements and a 0.5-m-long fibre in the second series of measurements, which allows us to dispense with a fibre-optic phase noise compensation system in the latter case. The beat signal is detected at a signal-to-noise ratio of 35 dB in a 1-kHz band.

In our case, the caesium fountain and a group of time keepers are situated ~1 km from the laboratory, where optical clocks based on neutral strontium atoms are located. The emission frequency of one of the hydrogen masers (HMs) in the group of time keepers of the caesium standard was transmitted through a 1.5-km-long uncompensated-noise fibre-optic link. The emission frequency of this hydrogen maser was used as a reference for the comparison scheme and all the instruments (synthesisers, frequency counters, etc.) used in the experiment.

The RF part of the scheme for comparing the strontium clock and caesium standard is realised as follows: The signal at the comb repetition frequency is detected by a 'fast' photodetector and amplified by a low-noise RF amplifier. Next, the signal is divided into two channels, one of which serves for direct f_{rep} measurements with a 5120A commercially available phase noise meter (Microsemi, USA), which ensures a measurement accuracy of 4×10^{-14} at an averaging time of 1 s. In the other channel, the signal is amplified, filtered and mixed in an RF mixer with a signal at a frequency of ~240 MHz from an SMB 100A RF signal generator (Rohde & Schwarz, Germany), to which the reference signal at a frequency of 10 MHz from the HM is fed. The difference signal after the mixer is again amplified, filtered and fed to one of the channels of an FXE dead-time-free counter (K+K, Germany), which ensures a relative accuracy of 3×10^{-13} at an averaging time of 1 s for frequency measurements up to 65 MHz. The measurement results from the counter and phase noise meter are read through a local network using a computer, which performs real-time information processing, stores new data, displays measurement results and informs if there is no stabilisation of the comb frequency f_{rep} to the clock laser frequency or the clock laser frequency to the atomic transition frequency.

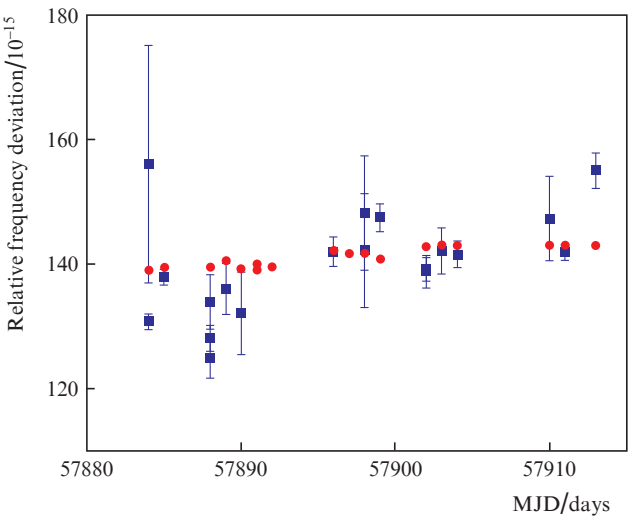

Figure 4. Results of comparing a strontium clock with a caesium standard with an HM in a group of time keepers. The circles represent the deviation of the HM frequency from the caesium standard frequency and the squares represent the deviation of the HM frequency from the clock frequency. During one day, we were able to perform several series of HM frequency measurements relative to the clock with different durations. The horizontal axis shows time in the form of the Modified Julian Date (MJD), in which a day begins at midnight, which corresponds to the commonly accepted time division into days (MJD = JD – 2 400 000.5, where JD is the Julian Date; e.g. MJD = 57 884 corresponds to 00:00 11 May 2017).

Thus, we constructed a system for comparing the strontium clock with a caesium standard using an HM in a group of time keepers. Figure 4 presents results of frequency measurements for an HM relative to the frequencies of a caesium fountain and strontium optical clock. It is worth noting that the time it takes for comparing the HM and caesium standard frequencies differs from that for comparing the HM and optical clock frequencies. The secondary cooling system operated continuously, but long-term strontium clock functioning was strongly influenced by failures in the system for stabilising the clock laser frequency to the atomic transition frequency due to the acoustic noise in the laboratory. Thus, comparisons were made at different instants of time and with different numbers of measurement points.

To improve the stability and increase the duration of continuous clock operation, we tested two algorithms for clock laser frequency stabilisation to the atomic transition frequency. We performed two series of experiments to examine long-term autonomous strontium clock operation. In the first series, the clock laser frequency was stabilised to the frequency of the $^1S_0$–$^3P_0$ atomic transition of ^{87}Sr atoms: to the maximum excitation probability P in the reconstructed spectrum of the atomic transition. The measurements were made for nine days and the duration of autonomous optical clock operation was 25 000 to 50 000 s (Fig. 5). We also achieved a record long continuous autonomous operation of the strontium clock and frequency comb: 250 000 s. One cause of the prolonged continuous optical clock operation is that the acoustic noise in the laboratory was reduced during the measurements. It is necessary however that the system retain its performance under routine conditions. To this end, we performed a second series of measurements using the latter

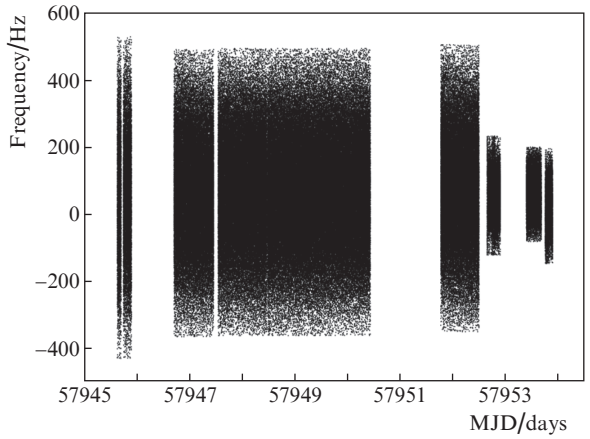

Figure 5. Results of prolonged clock laser frequency measurements. The data obtained starting at the second half of 57 952 MJD differ from the preceding data by a better signal-to-noise ratio of the beat frequency between the clock laser and femtosecond comb due to the use of the femtosecond regime of the comb with a higher power of the 698-nm mode. The vertical axis shows the difference between the magnitudes of the ^{87}Sr $^1S_0$–$^3P_0$ transition frequencies obtained in measurements relative to the HM frequency and the value recommended by CIPM: 429 228 004 229 873.2 Hz. The duration of the measurements during the time interval 57 947 to 57 950 MJD was ~250 000 s (with one brief absence of frequency comb stabilisation detected after 24 h of measurements) and was reached, in particular, through special measures to reduce the acoustic noise in the laboratory during the measurements.

algorithm described above, which is based on the fitting of the excitation probability (P) spectrum with a Lorentzian. In addition, we moved the frequency comb to a thermally stabilised room, together with the clock laser. This allowed us to resolve the problem of the loss of comb frequency (f_{rep}) stabilisation to the clock laser frequency due to the comb frequency drift. Figure 6 demonstrates the effectiveness of the algorithm used to stabilise the clock laser frequency to an atomic resonance. Autonomous strontium clock operation was ensured for 70 000 to 200 000 s without reducing the acoustic noise in the laboratory.

6. Conclusions

We have described approaches for resolving the problem of prolonged continuous autonomous operation of the ^{87}Sr optical clock. One approach is to abandon phase stabilisation of laser sources for secondary cooling of atoms. It is applicable in the case of stationary systems, which have no limitations on their dimensions. The other approach – laser stabilisation to an atomic resonance – is applicable to not only stationary but also transportable optical clocks [20, 29], which suffer from more acoustic noise. The use of these methods enabled nominal autonomous optical clock operation for several days.

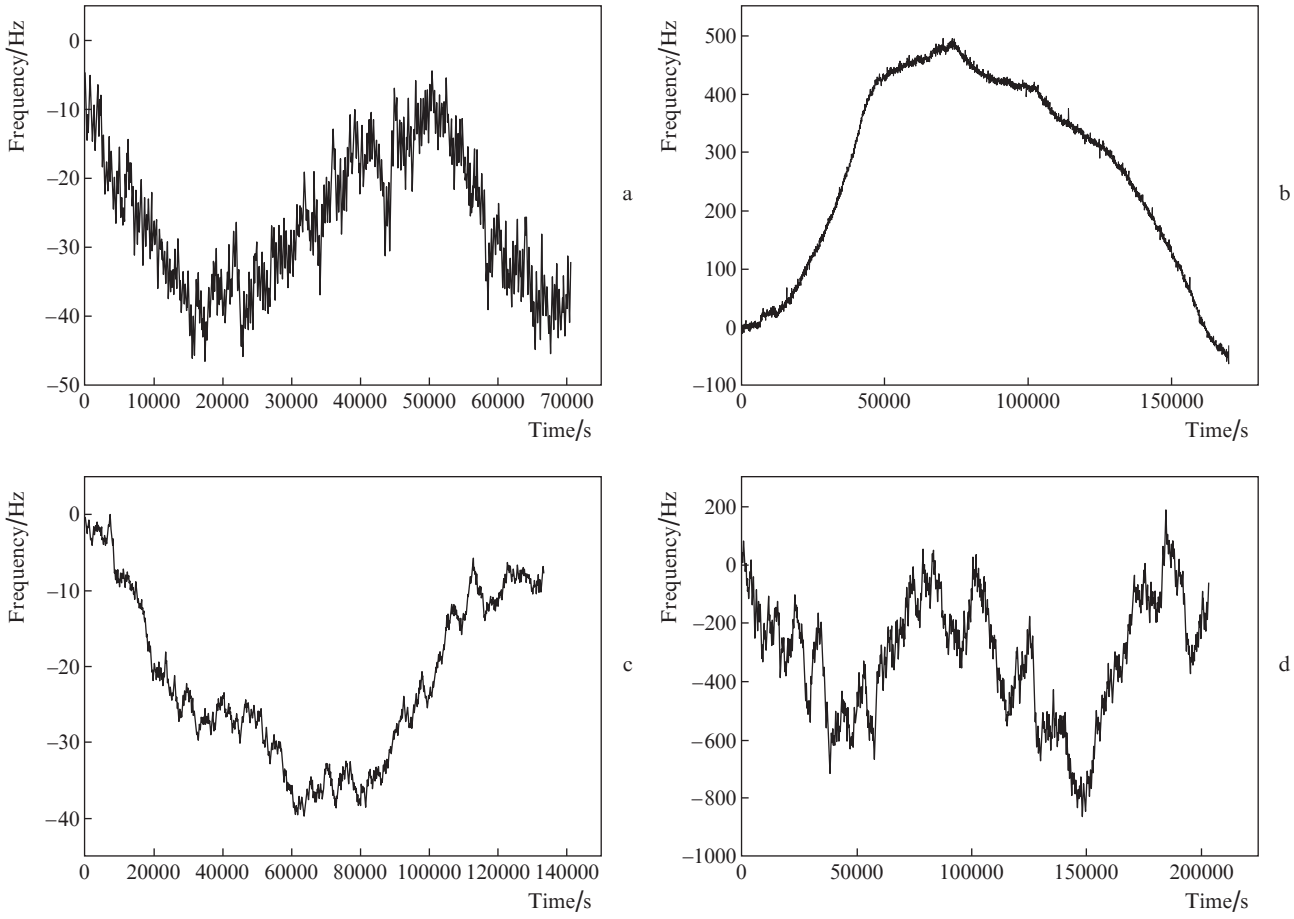

Figure 6. Demonstration of the effectiveness of the algorithm used to stabilise the clock laser frequency to the frequency of the ^{87}Sr $^1S_0$–$^3P_0$ transition by fitting the excitation probability with a Lorentzian at different spectral linewidths of the clock transition. The vertical axis shows the AOM-T correction frequency (Fig. 3) minus its linear drift. In panels a, b, c and d, the linewidths of the transition are 10, 10, 30 and 50 Hz, respectively.

References

1. Essen L., Parry J.V.L. *Nature*, **176**, 280 (1955).
2. Le Targat R. et al. *Nat. Commun*., **4**, 2109 (2013).
3. Rosenband T. et al. *Science*, **319**, 1808 (2008).
4. Huntemann N. et al. *Phys. Rev. Lett*., **113**, 210802 (2014).
5. Godun R.M. et al. *Phys. Rev. Lett*., **113**, 210801 (2014).
6. Altschul B. et al. *Adv. Space Res.*, **55**, 501 (2015).
7. Tarallo M.G. et al. *Phys. Rev. Lett*, **113** (2), 023005 (2014).
8. Derevianko A., Pospelov M. *Nat. Phys*., **10**, 933 (2014).
9. Dow J.M., Neilan R.E., Rizos C. *J. Geodyn*., **83**, 191 (2009).
10. Normile D., Clery D. *Science*, **333**, 1820 (2011).
11. Nicholson T.L. et al. *Nat. Commun*., **6**, 6896 (2015).
12. Huntemann N., Sanner C., Lipphardt B., Tamm C., Peik E. *Phys. Rev. Lett*., **116**, 063001 (2016).
13. Riehle F. *C. R. Phys*., **16**, 506 (2015).
14. Gill P. *Philos. Trans. R. Soc., A*, **369**, 4109 (2015).
15. Ushijima I., Takamoto M., Das M., Ohkubo T., Katori H. *Nat. Photonics*, **9**, 185 (2015).
16. Chou C.W., Hume D.B., Koelemeij J.C.J., Wineland D.J., Rosenband T. *Phys. Rev. Lett*., **104**, 070802 (2010).
17. Guéna J. et al. *IEEE Trans. Ultrason. Ferroelectr. Freq. Control*, **59**, 391 (2012).
18. Szymaniec K., Lea S.N., Liu K. *IEEE Trans. Ultrason. Ferroelectr. Freq. Control*, **61**, 203 (2014).
19. Lisdat C. et al. *Nat. Commun*., **7**, 12443 (2016).
20. Koller S.B. et al. *Phys. Rev. Lett*., **118** (7), 073601 (2017).
21. Hachisu H., Ido T. *Jpn. J. Appl. Phys*., **54** (11), 112401 (2015).
22. Dörscher S., Häfner S., Gerginov V., Weyers S., Lipphardt B., Riehle F., Sterr U., Lisdat C., Grebing C., Al Masoudi A. arXiv:1511.03888 (2015).
23. Strelkin S.A., Khabarova K.Yu., Galyshev A.A., Berdasov O.I., Gribov A.Yu., Kolachevsky N.N., Slyusarev S.N. *Zh. Eksp. Teor. Fiz*., **148** (1), 25 (2015).
24. Berdasov O.I., Gribov A.Yu., Belotelov G.S., Pal'chikov V.G., Strelkin S.A., Khabarova K.Yu., Kolachevsky N.N., Slyusarev S.N. *Quantum Electron*., **47** (5), 400 (2017) [*Kvantovaya Elektron*., **47** (5), 400 (2017)].
25. Barwood G., Gao K., Gill P., Huang G., Klein H. *IEEE Trans. Instrum. Meas*., **50** (2), 543 (2001).
26. Bernard J.E., Marmet L., Madej A.A. *Opt. Commun*., **150** (1–6), 170 (1998).
27. Peik E., Schneider T., Tamm C. *J. Phys. B: At. Mol. Opt. Phys*., **39** (1), 145 (2006).
28. Telle H.R., Steinmeyer G., Dunlop A.E., Stenger J., Sutter D.H., Keller U. *Appl. Phys. B*, **69** (4), 327 (1999).
29. Poli N. et al. *Appl. Phys. B*., **117** (4), 1107 (2014).